Vertical transport through Landau levels in a GaAs/$Al_xGa_{1-x}As$ superlattice in the presence of a parallel magnetic field

F. Piazza and L. Pavesi
Dipartimento di Fisica, Università di Trento, I-38050 Povo, Trento, Italy

H. Cruz
Departamento de Física Fundamental y Experimental, Universidad de La Laguna, 38204 La Laguna, Spain

M. Micovic and C. Mendoça
Laboratorio TASC-Istituto Nazionale di Fisica della Materia, Area di Ricerca, Padriciano 99, 34012 Trieste, Italy

(Received 11 March 1992; revised manuscript received 25 September 1992)

Vertical transport through a short-period superlattice in the presence of a parallel magnetic field has been measured with an all-optical technique by use of an enlarged well imbedded in a superlattice. Magnetic-field and power dependence of the transport have been found and interpreted by computing the quasi-Fermi-level of the photoexcited electron gas via the calculation of the density of states of a superlattice in a parallel magnetic field. The vertical transport is reduced by the formation of disorder-broadened Landau levels. By measuring photoluminescence excitation spectra, we have been able to demonstrate the energy dependence of transport through Landau levels.

I. INTRODUCTION

An external magnetic field B transforms the steplike density of states (DOS) of a two-dimensional electron gas in a series of Landau levels.[1] This influences the electron conduction in semiconductor heterostructures at low temperature. If the Fermi energy E_F coincides with a Landau level the electron gas conducts as in a metal. If E_F is between two Landau levels the system behaves like an insulator. In real systems, the disorder induced by impurities, interface defects, etc., broadens the Landau levels. A computer simulation was performed by Ando in Ref. 2 in order to calculate the broadening of Landau levels and the localization length (i.e., the distance over which the wave function of localized states decays) of the states. It was shown there that localized states which do not contribute to the transport are formed in the tails of each broadened Landau level. Therefore, a two-dimensional electron gas in a magnetic field has an energy spectrum consisting of a succession of extended and localized states. This explains oscillatory effects in the resistivity of two-dimensional systems, like the quantum Hall effect.[3]

Magneto-optical measurements in heterostructures are usually performed to obtain the binding energy of the excitons,[4] or to check the assignment of the optical structures in photoluminescence excitation spectra.[5] Some measurements concerning the vertical transport through superlattice minibands in the presence of a magnetic field have been performed.[6,7]

In this paper, using an all-optical method, we study the formation of Landau levels in short-period superlattices, and the effect of the disorder-induced localization in the tails of Landau levels on vertical transport. The higher-energy resolution of optical techniques with respect to electrical techniques allows the measurement of the energy dependence of the transport. The samples we used consist of two GaAs/$Al_xGa_{1-x}As$ ($x = 0.3$) superlattices (SL) which include an enlarged well (EW). The EW acts as a marker of the carrier motion.[8] In Sec. II we present the photoluminescence result and in Sec. III we report the calculation of the DOS of a SL under a magnetic field parallel to the growth direction and discuss the formation of Landau levels in order to interpret our experimental results.

II. EXPERIMENTAL DATA

The sample structure is as follows: 1-μm thick buffer layer, 50 nm of an $Al_xGa_{1-x}As$ layer, a superlattice, an enlarged well, a superlattice identical to the previous one, 50 nm of an $Al_xGa_{1-x}As$ layer, and a 5-nm thick GaAs caplayer in order to prevent oxidation of $Al_xGa_{1-x}As$. The two 50-nm thick $Al_xGa_{1-x}As$ layers were grown to minimize diffusion of the photogenerated carriers into the buffer layer and to the surface. The active region of the sample consists of two symmetric superlattices which sandwich an EW. The different samples have a 18/18 superlattice (18-Å wide wells and barriers, x=0.3) with a 40-Å wide EW (sample 1), and a 30/30 superlattice with a 60-Å wide EW (sample 2). The number of periods for each SL is 49. These are typical structures used in vertical transport measurements by optical techniques.[8] In fact, the low-temperature photoluminescence spectrum of such samples is characterized by two distinct emission lines due to excitonic recombinations in the SL or in the EW spatial regions. Due to the small thickness of the EW, its photoluminescence is mainly due to the recombination of electron-hole pairs that have been previously

photoexcited in the SL region and have then moved into the EW itself.

The experiments have been performed in a backscattering geometry using a Pyridhine 2 dye laser pumped by an argon laser. The samples were placed in a cryostat equipped with a superconductor magnet and were immersed in liquid helium (sample temperature is equal to 4.2 K). The photoluminescence spectra were analyzed with a double monochromator and recorded by photon counting techniques using a cooled GaAs photomultiplier.

On samples 1 and 2 we have measured the luminescence spectra varying the magnetic field from 0 to 4.4 T. The energy positions of the SL and EW emission lines and their widths did not depend on the strength of the magnetic field. This means that the PL transitions are of excitonic origin because the excitons show a weak diamagnetic shift in magnetic field while e-h pairs show a large shift.[4] In Fig. 1, we show the magnetic-field dependence of the quantity $R = I_{EW}/(I_{SL} + I_{EW})$, where I_{EW} and I_{SL} are the integrated luminescence intensities from the EW and the SL, respectively. R is proportional to the number of carriers which reach the EW starting from the SL. Two different excitation intensities ($J = 2$ or 80 W/cm^2) were used. One can see that the R values decrease with increasing the magnetic field. Both samples 1 and 2 present the same power dependence: for high J the R curve is convex [see Figs. 1(a) and 1(c)] while for low J the R curve is concave [see Figs. 1(b) and 1(d)]. The relative variations of R in Figs. 1(b) (sample 1 low J) and 1(c) (sample 2 high J) are much stronger than the R variations in Figs. 1(a) (sample 1 high J) and 1(d) (sample 2 low J). As already discussed and demonstrated in our previous works,[9] the influence of variations in the superlattice absorption coefficients on R is negligible. $\alpha \simeq 2 \times 10^4$ cm^{-1} in superlattices, which corresponds to a great penetration depth of the laser light ($\simeq$ 500 nm) and, hence, to a quite homogeneous excitation of the superlattice.

A series of excitation spectra for different magnetic fields from 0 to 4 T is presented for sample 1 in Fig. 2 and for sample 2 in Fig. 5. Each excitation spectrum was performed by collecting the luminescence from the SL emission peak and from the EW emission peak. The sum of the two excitation spectra is indicative of the joint density of states. The excitation spectrum of SL provides information on the states which do not permit an efficient transport through the SL. On the contrary, the excitation spectrum of the EW provides information on the states which allow an efficient transport.

For B=0 T, the excitation spectra of sample 1 do not show any excitonic resonance (see Fig. 2). We think that this is so because in a 3.6-nm period superlattice the interface disorder broadens the excitonic states so that these merge into the continuum of e-h pairs.[10] Thus the joint density of states is dominated by free e-h pair tran-

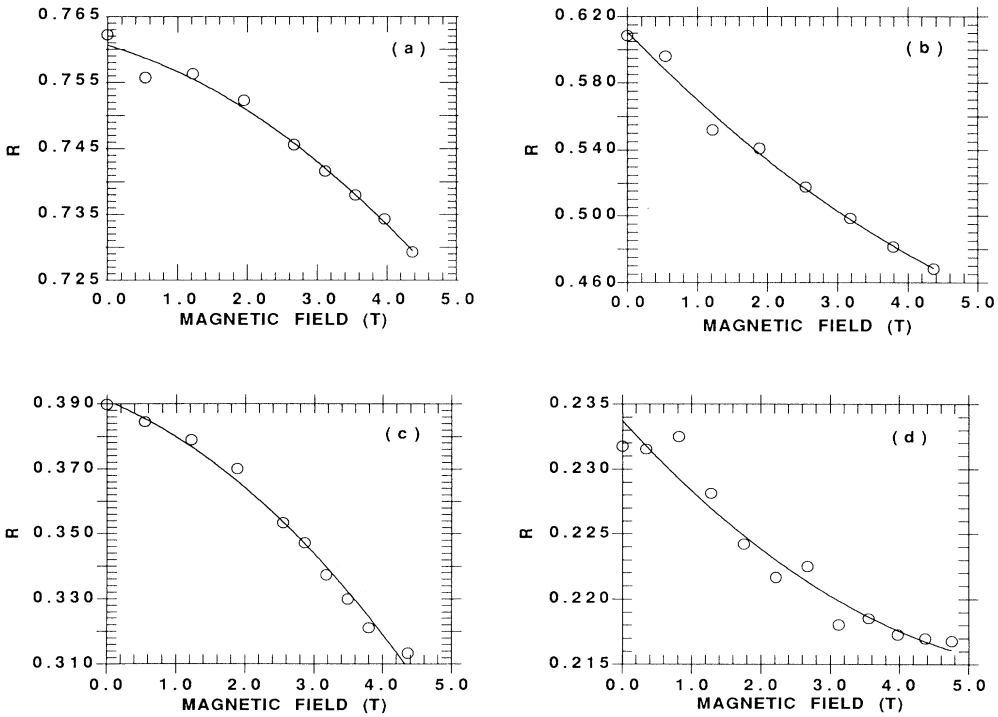

FIG. 1. R=$I_{EW}/(I_{EW} + I_{SL})$ as a function of the magnetic field for samples 1 [panels (a) and (b)] and 2 [panels (c) and (d)]; I_{EW} is the integrated photoluminescence emission from the enlarged well and I_{SL} from the superlattice. Panels (a) and (c) are measured with an excitation power of 80 W/cm^2 and panels (b) and (d) with 2 W/cm^2. Continuous lines are used to demonstrate the concavity or convexity of the plots.

sitions. By increasing the magnetic field two peaks grow up at 1.735 eV in the SL excitation spectrum, and at 1.738 eV in the EW excitation spectrum, respectively.

In Fig. 3 we show the magnetic-field dependence of the ratio

$$R'(\hbar\omega) = \frac{I_{\rm EW}(\hbar\omega)}{I_{\rm EW}(\hbar\omega) + I_{\rm SL}(\hbar\omega)}\ , \qquad (1)$$

where $I_{\rm EW}$ and $I_{\rm SL}$ are the intensity of the luminescence from the EW and from the SL for an excitation energy $\hbar\omega$, respectively. The quantity R' is connected with the transport efficiency, as discussed above. By increasing B a well-defined peak, 4 meV wide, with two deep minima on its sides develops in R' at $\hbar\omega \simeq 1.74$ eV. In Fig. 4, the energy position of the R' peak is shown for different values of B. The dependence of the R' peak on B is linear with a slope of 0.9 ± 0.1 meV/T. The constant term, which gives the position of the R' peak for zero magnetic field, is 1.736 ± 0.001 eV. A similar structure in R' is observed at higher energies ($\simeq$ 1.75 eV). Its dependence on B is linear with a slope of 1.4 ± 0.3 meV/T. The constant term is 1.742 ± 0.001 eV.

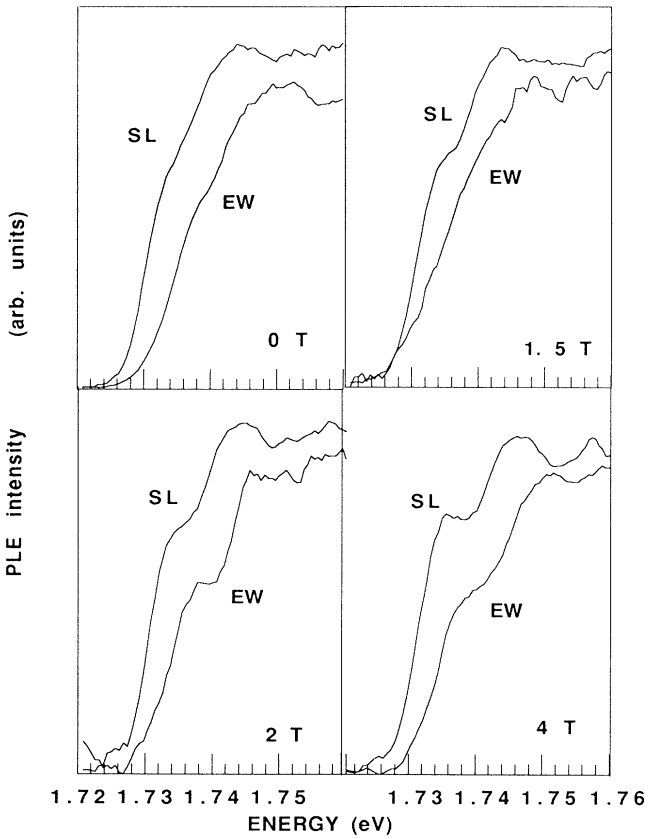

FIG. 2. Series of excitation spectra for sample 1 for magnetic fields of 0 , 1.5, 2.0, and 4.0 T. The luminescence from the enlarged well and the luminescence from the superlattice are indicated with EW and SL, respectively. Each spectrum is normalized to its maximum. The relative intensity can be deduced from Fig. 1. An excitation power of 1 W/cm^2 was used.

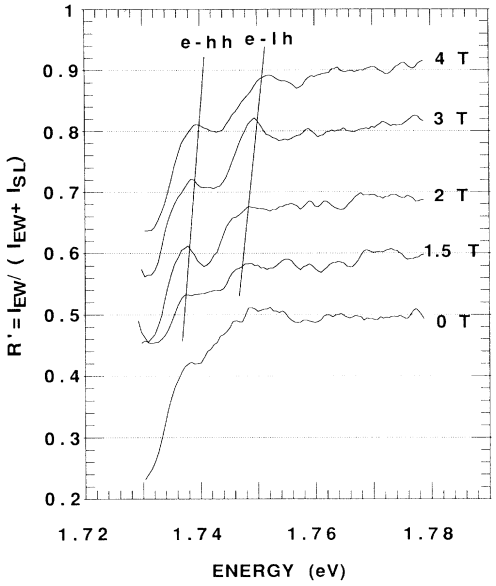

FIG. 3. Magnetic-field (B) dependence of $R'(\hbar\omega) = I_{\rm EW}(\hbar\omega)/[I_{\rm EW}(\hbar\omega) + I_{\rm SL}(\hbar\omega)]$ (continuous line), where $I_{\rm EW}(\hbar\omega)$ is the excitation spectrum from the enlarged well and $I_{\rm SL}(\hbar\omega)$ from the superlattice. Each R' curve has been shifted by 0.1. e-hh and e-lh refer to electron heavy-hole or electron light-hole band edge, respectively. The data refer to sample 1.

The excitation spectra of sample 2 are shown in Fig. 5. The SL excitation spectra present two resonances at 1.704 eV and 1.720 eV for B=0 T. They correspond to the absorption of the heavy-hole (HH) and light-hole (LH) excitons. The spectral position of these features does not change as we increase B. In the EW excitation spectra the HH resonance is missing due to the absence of transport associated with HH excitons in these superlattices.[11,10] The steplike shoulder at 1.71 eV is associated with the HH excitons continuum (resonant excitation of free-electron–heavy-hole pairs). The difference between this shoulder and the HH resonance in the SL excitation spectra correlates well with the 5 meV binding energy of HH excitons in 60-Å period superlattices.[12] By increasing B the shoulder smears out, but there is no evidence of the formation of the first Landau level for e-h pairs as shown in Fig. 2 for sample 1. At higher energies the LH resonance is observed. LH excitons, due to the smaller mass with respect to HH excitons, could move through the superlattice miniband and hence contribute to the EW luminescence as well. The LH resonance does not shift as a function of B. Such a difference in the behavior of excitons and of e-h pairs in a magnetic field has been deeply discussed in Ref. 5.

III. DISCUSSION

Because in Landau levels the transport depends on the position of the quasi-Fermi-level, $E^e_{\rm QF}$, we have calcu-

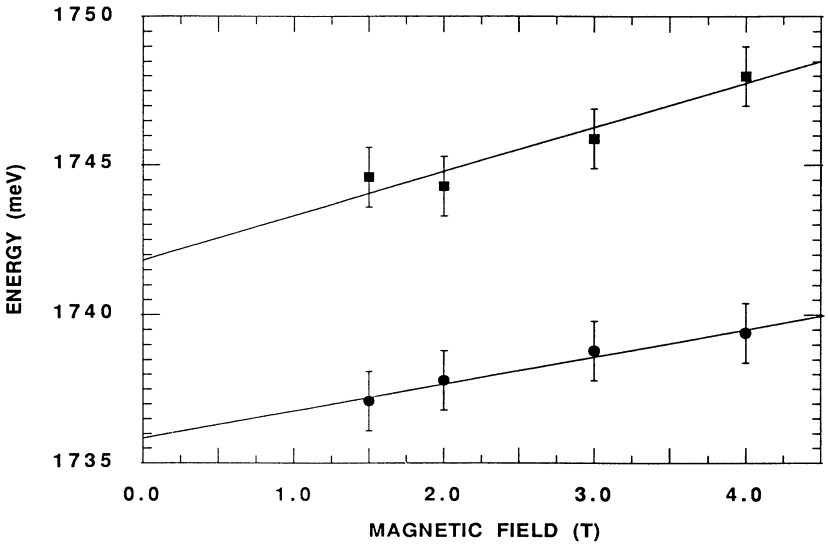

FIG. 4. Spectral position of the two peaks in R' (defined in the caption of Fig. 3) as a function of the magnetic field. The continuous lines are linear fits. The resulting equations are $(1736 + 0.9B)$ meV (upper curve) and $(1742 + 1.4B)$ meV (lower curve), where B is measured in units of Tesla. The data refer to sample 1.

lated $E^e_{\rm QF}$ for electrons. For simplicity we neglect the formation of the excitons in our calculation. $E^e_{\rm QF}$ is the solution of the integral equation[13]

$$n_{\rm tot} = \int_{E_{\rm cond}}^{\infty} \frac{1}{\exp(E - E^e_{\rm QF}) + 1} \rho_c(E)\, dE\,, \qquad (2)$$

where $n_{\rm tot}$ is the total number of photoexcited electrons in the miniband, $E_{\rm cond}$ is the bottom of the SL conduction miniband, and $\rho_c(E)$ is the electron density of states.

We have computed $\rho_c(E)$ using disorder-broadened Landau level centered at the energy E_l:

$$E_l = E_m + \hbar\omega_c\left(n + \tfrac{1}{2}\right) + g_e m_z \mu_b B\,, \qquad (3)$$

where E_m is the energy level for the motion along the growth direction, ω_c is the cyclotronic frequency, eB/m^*, calculated using the GaAs effective mass, n is the Landau-level index, g_e is the g value for the electron, m_z is the component along the growth axis of the intrinsic angular momentum of the electron, and μ_b is the Bohr magneton. The energy levels E_m of a superlattice in a magnetic field B applied parallel to the growth direction have been computed by the transfer-matrix method[14] which is based on the independent particle approximation and on the effective mass and envelope function approximations.[1] As shown in Ref. 15, the magnetic energy due to the electron spin is negligible in GaAs. Neglecting this term, the electron density of states becomes

$$\rho_c(E) = \frac{eB}{2\pi\hbar\sigma}\sqrt{\frac{2}{\pi}}\sum_{m,n}\exp\{-[\,E_m + \hbar\omega_c(n + 1/2) - E]^2/\sigma^2\}, \qquad (4)$$

where the index m runs over the superlattice miniband levels, and $0 \le n \le \infty$ is the Landau-level index. σ takes into account the broadening due to the disorder. The value of σ is almost independent on the quantum number

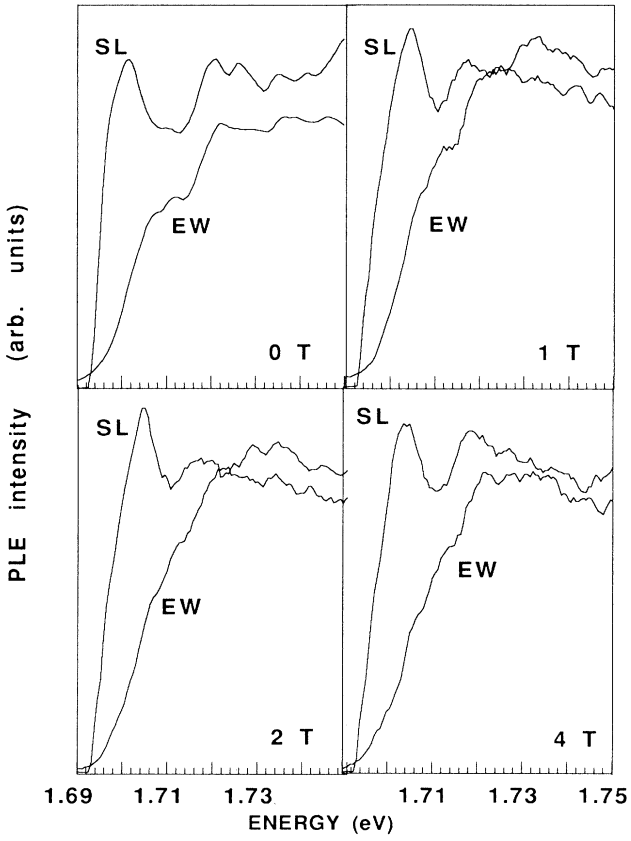

FIG. 5. Series of excitation spectra for sample 2 for magnetic fields of 0, 1.0, 2.0, and 4.0 T. The luminescence from the enlarged well and the luminescence from the superlattice are indicated with EW and SL, respectively. Each spectrum is normalized to its maximum. The relative intensity can be deduced from Fig. 2. An excitation power of 1 W/cm^2 was used.

$n.^2$ $\rho_c(E)$ has the two-dimensional density of states as limit for $B \to 0$.

The condition for a zero-dimensional DOS (appearance of well-defined Landau levels) is that $\hbar\omega_c > \sigma$. This condition is easier to reach for electrons than for heavy holes, which have a ten time heavier mass. Consequently, in the magnetic-field intensity range from 0 to 5 T at which the measurements were performed the magnetic confinement effects are dominated by the electrons. This assumption is supported by the findings of Ref. 4 where a linear dependence on B of the Landau energy levels has been measured by photoluminescence excitation spectroscopy. The slope of the linear relation is fitted using the electron cyclotron energy only, although the measure involves optical transitions between electron and heavy holes.

According to the model of Ref. 2, a disorder-broadened Landau level is formed by extended states for energies in the center of the level and by localized states for energies in the tails. The extended states have localization length comparable with the sample size, while the localization length for localized states markedly decreases for energies far from the center of the Landau level. Moving from the center of the Landau level to the tails the localization length of the states decreases, at the beginning slowly and then sharply when a critical energy that marks the border between the localized and the extended states is reached (see, e.g., Fig. 3 of Ref. 2). Carriers occupy these states following a Fermi-Dirac distribution. Only those carriers which occupy partially filled states contribute to the transport. These states differ from E^e_{QF} less than kT where k is Boltzmann's constant and T the carrier temperature. At 4 K, $kT \approx 0.34$ meV.

In Figure 6(a), we show the Landau-level energy E_l and the quasi-Fermi-level E^e_{QF} as a function of B for two different values of J: 2 and 80 W/cm^2. In the calculation, σ=2.5 meV. This value of σ has been computed from the broadening of the R' resonance (see Fig. 3). The degeneracy of each Landau level depends on B and it is about 4.2x10^{10} cm^{-2} T^{-1}. The sheet density of photoexcited electrons for J=80 W/cm^2 is about 2x10^{10} cm^{-2}. For $B > 1.5$ T and σ=2.5 meV, these conditions yield $\hbar\omega_c > \sigma$, no Landau levels overlap, and only the first Landau level is occupied [Fig. 6(a)].

Let us now discuss how the evolution of E^e_{QF} with B explains our experimental results of Fig. 1. We have found in Sec. II that (i) the transport, as measured by R, decreases as B increases, (ii) for high J the transport is larger than for low J, (iii) the R dependence on B is convex for high J while it is concave for low J, and (iv) the relative change in R is larger for low J than for high J for the sample with high R and the relative change is larger for low J than for high J for the sample with a low R.

Item (i) is explained by the fact that by increasing B, the energy difference between the center of Landau level E_l and E^e_{QF} increases due to a larger degeneracy of the single state moving away from E_l. Consequently, a smaller number of extended states is occupied and the transport decreases. Regarding item (ii), when J is increased, E^e_{QF} approaches E_l, more extended states are occupied, and R increases. To explain item (iii) we have to compare the value of kT with the broadening of the Landau level. We observe that, for high J, a shift of E^e_{QF} due to a variation in B changes weakly the ratio between the extended and localized states involved in the transport and, hence, R. In fact the states involved in the transport are in a small energy interval around E^e_{QF} and E^e_{QF} shifts near the center of the Landau level where the states are extended. By decreasing J, E^e_{QF} is in the tails of the Landau level and an increase in B makes R decrease appreciably because E^e_{QF} moves from a region of extended states to a region of localized states [see Fig. 6(a)].

This explanation is further supported by a simple calculation of the number n' of electrons which occupy extended states and participate in the transport [see

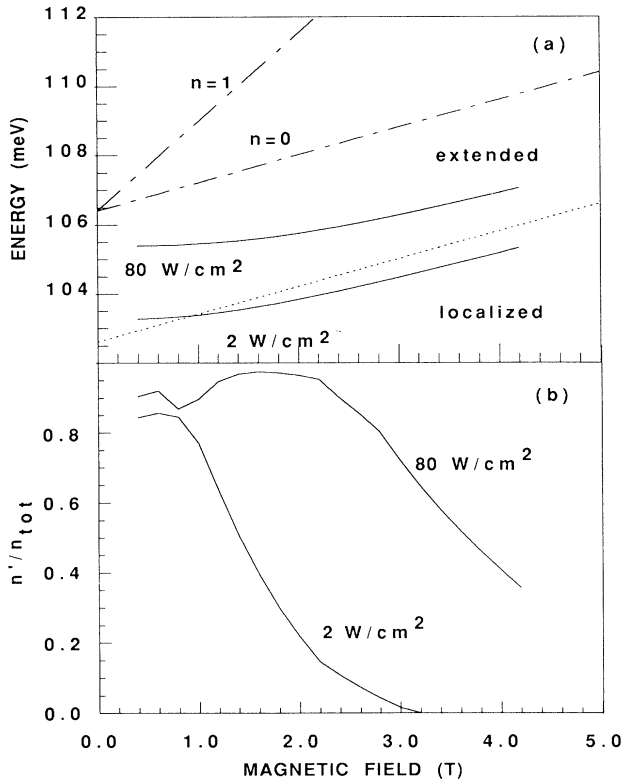

FIG. 6. Panel (a): Computed quasi-Fermi energy E^e_{QF} (full lines) for two excitation powers J_{exc} = 2 mW/cm^2 and J = 80 mW/cm^2, respectively. The n=0 and n=1 Landau levels are indicated by the dashed-dotted lines. The critical energy that separates the extended states from the localized states in the first Landau level is indicated by the dotted line. A disorder broadening of σ= 2.5 meV is used in the calculations. The relation between J_{exc}, measured before the cryostat windows, and the total photoexcited carrier density n_{tot} is $n_{tot} = \mathcal{R}J_{exc}S/(\hbar\omega)\,[1-\exp(-\alpha L)]\,\tau$, where $\mathcal{R}$=0.4 takes into account the reflection of the cryostat windows and the sample surface, S=1.0×10^{-4} cm^2 is the excitation surface, $\alpha = 2\times10^4$ cm^{-1}, and $\tau = 5\times10^{-10}$ s. Panel (b): Computed ratio between the number n' of carriers that occupy extended states that differ for less than kT from E^e_{QF} and n_{tot}. The calculation was performed for excitation powers J_{exc} = 2 and 80 mW/cm^2 as indicated.

Fig. 6(b)]. The ratio $n'/n_{\rm tot}$ is a rough approximation to R. We assume that n' is given by the electrons which are in a small energy interval $[E^e_{\rm QF}+kT, E^e_{\rm QF}-kT]$ around $E^e_{\rm QF}$. The critical energy which separates the extended and localized states has been assumed to be $E_l \pm 1.5\sigma$. The model assumes an infinite localization length for extended states and a zero localization length for localized states. As one can see in Fig. 6(b) this model reproduces qualitatively the measured R curves. In particular, $n'/n_{\rm tot}$ has a concave shape for J=2 W/cm^2 and a convex shape for J=80 W/cm^2. For $B \leq 1.5$ T, $n'/n_{\rm tot}$ has oscillations due to the fact that several Landau levels are occupied, they merge into a continuum of states, and $\rho_c(E)$ tends to the two-dimensional limit. The large value of the critical energy used ($E_l - 1.5\sigma$) is a consequence of the drastic approximation used for the energy dependence of the localization length. Lower values for the critical energy cannot reproduce the convex shape at high J. More sophisticated models are necessary in order to infer from these experimental data a reliable value for the critical energy of Landau levels.

Item (iv) is explained by the different values of the critical energy for the two samples. Sample 1 has a larger transport efficiency than sample 2 at B=0 T which indicates a lower disorder extent. In sample 1, which has a large energy difference between the critical energy and the Landau-level energy, and for high J, the $E^e_{\rm QF}$ moves in an energy region of mainly extended states when B increases. Consequently, R changes weakly. On the other hand, in sample 2, which has a small energy difference between the critical energy and the Landau-level energy, and for high J, the $E^e_{\rm QF}$ shifts from about E_l through the critical energy when B increases. Hence, R changes strongly. By varying B when J is low, $E^e_{\rm QF}$ moves through the critical energy for sample 1 and in an energy region of mainly localized states for sample 2. Thus R varies strongly for sample 1 and weakly for sample 2, although the absolute value is much lower for sample 2 than for sample 1.

The interpretation of the excitation spectra of sample 1 is possible considering only free carrier recombinations, and neglecting excitonic effects. There is no experimental evidence of the formation of excitons in the excitation spectra (Fig. 2). It is already known in the literature that for short-period superlattices the transport is due to the ambipolar motion of electron-hole pairs through the superlattice minibands.[16] We think that the peaks, which develop in R' with increasing B, are due to the formation of the first Landau level in the joint density of states both for electron heavy-hole (e-hh) pair (peak at 1.736 eV) and for electron light-hole (e-lh) pair (peak at 1.742 eV). As discussed above, a disorder-broadened Landau level has extended states at the center and localized states in the tails. Hence in this energy region, $R'(\hbar\omega)$ has minima (no transport because the excitation is resonant with localized states) at the sides of a pronounced maximum (efficient transport because excitation is resonant with extended states) (Fig. 3). This interpretation is confirmed by the energy dependence of the $R'(\hbar\omega)$ peaks on B. By using the simple model discussed above the energy shift of the first Landau level is found to have a slope equal to $(1/2\ \hbar\omega_c/{\rm B})=(\hbar e/m^*)$, where m^* is the reduced mass of the moving particle and e the unit charge. Table I reports a comparison of the experimental and computed values for moving e-hh and e-lh pairs. The agreement is good considering the error bar in the experimental data and the very simple model used. If this picture is correct (e-hh and e-lh related Landau levels) the constant term in the R' peak dependence on B gives the energy $\mathrm{E}_{e\text{-hh/lh}}=\mathrm{E}_g+\mathrm{E}_e+\mathrm{E}_{\rm hh/lh}$, where E_e and $\mathrm{E}_{\rm hh/lh}$ are the miniband edge of the electronic and heavy-hole or light-hole minibands, respectively, and E_g is the GaAs band gap. Consequently, the light–heavy-hole miniband splitting is $\mathrm{E}_{e\text{-hh}}$-$\mathrm{E}_{e\text{-lh}}$=(1.742−1.736) eV $\simeq$ 6 meV. For a single 18-Å thick quantum well the light–heavy-hole splitting is 30 meV,[1] while for a 18/20 short-period superlattice calculations and experimental data indicate a lower value ($\simeq$ 8meV).[12]

No similar effects are observed on the excitation spectra of sample 2. We think that the main reason for this is the appearance of well resolved excitonic resonances. In sample 1 the transport is mainly affected by the disorder while in sample 2 the transport is limited by the formation of excitons.[10] In a 30/30 superlattice (sample 2) the first heavy-hole miniband is very thin (about 2 meV), a weak coupling exists among different wells, and the heavy holes are confined in the well regions. The HH exciton motion is strongly limited by the heavy-hole confinement. Increasing the magnetic field no preferential energy regions for the transport develops in the HH exciton resonance. In addition, excitons have a weak diamagnetic behavior in a magnetic field. Thus their spectral positions depend on B very slightly and higher magnetic fields are needed to measure the weak diamagnetic shift.[4,5]

We note that the interpretation of the experimental data for R discussed previously is valid for both the 18/18 and the 30/30 superlattices although excitons form

TABLE I. Computed magnetic-field shift ($1/2\ \hbar\omega_c/B$) of the first Landau level. The following particles have been considered: e, free electrons; e-hh, coupled electron heavy-hole pairs (the effective mass of the pair is equal to the reduced e-hh effective mass); e-lh, coupled electron light-hole pair. The effective mass is given in units of the electron mass in vacuum, m_0. The experimental column refers to the data shown in Fig. 4 for sample 1.

Particle	Effective mass (m_0)	$1/2\ \hbar\omega_c$/B (meV/T)	Experimental (meV/T)
e	0.065	0.81	
e-hh	0.059	0.89	0.9±0.1
e-lh	0.037	1.42	1.4 ±0.3

clearly in the 30/30 superlattice. The fact is that the transport is mainly due to free *e-h* pairs as evidenced by the difference between the SL and the EW excitation spectra shown in Fig. 5.

IV. CONCLUSIONS

We have measured the transport properties of *e-h* pairs through superlattice miniband states in a parallel magnetic field. The *e-h* pair current decreases by increasing the magnetic field due to the formation of disorder–broadened Landau levels. The position of the quasi-Fermi-level in the broadened Landau level drives the transport. Energy sensitive measurements directly demonstrate the formation of extended states in the center and of localized states in the tails of the Landau levels in very short-period superlattices. The formation of excitons complicates this simple picture.

[1]G. Bastard, *Wave Mechanics Applied to Semiconductors Heterostructures* (Les Éditions de Physique, Paris, 1988).
[2]T. Ando, J. Phys. Soc. Jpn. **52**, 1740 (1982).
[3]K. von Klitzing, Festkörperprobleme **30**, 25 (1990).
[4]J. C. Maan, A. Fasolino, G. Belle, M. Altarelli, and K. Ploog, Physica B **127**, 426 (1984).
[5]B. Deveaud, A. Chomette, F. Clerot, A. Regreny, R. Romestain, J. C. Maan, G. Bastard, H. Chu, and Y. C. Chang, in *Spectroscopy of Semiconductor Heterostructures*, Vol. 206 of *NATO Advanced Study Institute, Series B: Physics*, edited by G. Fasol, A. Fasolino, and P. Lugli (Plenum, New York, 1989), p. 391.
[6]P. S. Kop'ev, R. A. Suris, I. N. Uraltsev, and A. M. Vasiliev, Solid State Commun. **72**, 401 (1989).
[7]B. J. Skromme, R. Bhat, M. A. Koza, S. A. Schwarz, T. S. Ravi, and D. M. Hwang, Phys. Rev. Lett. **65**, 2050 (1990).
[8]A. Chomette, B. Deveaud, J. Y. Emery, and A. Regreny, Superlatt. Microstruct. **1**, 201 (1985).
[9]E. Tuncel, L. Pavesi, F. Morier-Genoud, D. Martin, and F. K. Reinhart, Phys. Rev. B **38**, 1597 (1988).
[10]F. Piazza, L. Pavesi, A. Vinattieri, J. Pastor and M. Colocci (unpublished).
[11]L. Pavesi and F. K. Reinhart, Phys. Rev. B **42**, 11 362 (1990).
[12]A. Chomette, B. Lambert, B. Deveaud, F. Clerot, A. Regreny, and G. Bastard, Europhys. Lett. **4**, 461 (1987).
[13]R. L. W. Zawadzki, Solid State Commun. **50**, 537 (1984).
[14]H. Cruz, F. Piazza, and L. Pavesi, Semicond. Sci. Technol. (to be published).
[15]D. Bimberg, Phys. Rev. B **18**, 1794 (1990).
[16]B. Deveaud, J. Shah, T. C. Damen, B. Lambert, and A. Regreny, Phys. Rev. Lett. **58**, 2582 (1987).